Correlation Among Crystalline Morphology of PEEK, Interface Bond Strength, and In-Plane Mechanical Properties of Carbon/PEEK Composites

SHANG-LIN GAO, JANG-KYO KIM

Department of Mechanical Engineering, Hong Kong University of Science and Technology, Clear Water Bay, Hong Kong

Received 26 March 2001; accepted 29 May 2001

ABSTRACT: The effect of the cooling rate on in-plane and interlaminar properties of carbon fiber/semicrystalline PEEK matrix composites was studied. Strengths and moduli were measured in tension, flexure, and interlaminar shear, all of which were shown to correlate, to different degrees, with the fiber–matrix interface adhesion and the bulk matrix properties. The in-plane and interlaminar properties, in general, increased with a decreasing cooling rate, which was attributed to changes in the failure mechanism from adhesive failure involving fiber–matrix interface debonding at high cooling rates to matrix-dominant cohesive failure at low cooling rates. The present study demonstrates that the mechanical properties of semicrystalline thermoplastic composites can be tailored for desired applications by controlling the processing conditions, especially the cooling rate. © 2002 Wiley Periodicals, Inc. J Appl Polym Sci 84: 1155–1167, 2002; DOI 10.1002/app.10406

Key words: cooling rate; crystallinity; mechanical properties; interlaminar shear strength; carbon fiber/PEEK composite; interface; fracture

INTRODUCTION

The sensitivity of the mechanical behavior of semicrystalline polymers, and the composites made therefrom, to crystallinity and crystalline morphology has long been known. Reviews on this topic have been presented with some useful mechanical property data.[1,2] The presence of carbon fibers within the semicrystalline matrix induces preferential nucleation and growth of crystallites perpendicular to the fiber surfaces, that is, transcrystallites, which, in turn, have a considerable influence on the interphase interaction between the fiber and matrix and the mechanical properties of the composites.[3,4] There is substantial evidence that transcrystallization further improves the fiber–matrix interface adhesion and the mechanical properties of the interphase by preventing the formation of a weak layer containing many impurities.[5,6] These crystalline characteristics and the interactions at the interphase region are, in turn, determined by a number of factors, including composite processing conditions such as molding temperature, cooling rate, holding time and temperature, and annealing conditions.[7–18]

The cooling rate, with which the present article is mainly concerned, in particular, has shown a significant influence on phenomena taking place at the interphase region. Experiments over a wide range of cooling rates from 1 to 2000°C/min reveal

Correspondence to: J.-K. Kim (mejkkim@ust.hk).

Contract grant sponsor: Research Grant Council; contract grant number: CERG HKUST719/95E.

Contract grant sponsor: Hong Kong University of Science & Technology (HKUST); contract grant number: AoE97/98.EG14.

Journal of Applied Polymer Science, Vol. 84, 1155–1167 (2002)

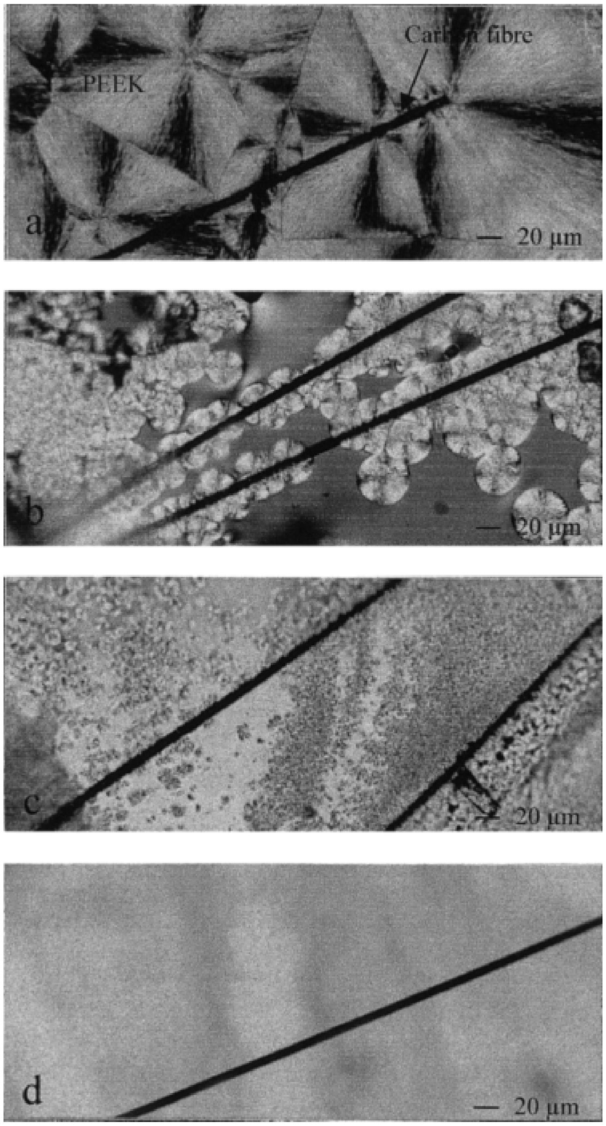

Figure 1 Micrographs of PEEK crystalline morphology around isolated carbon fibers at cooling rates of (a) 1°C/min, (b) 200°C/min, (c) 1000°C/min, and (d) 2000°C/min.

close correlations among the degree of crystallinity in the PEEK resin, crystalline morphology at the fiber–matrix interphase region, the interface bond strength, as well as the interlaminar fracture and impact damage resistance of composites.[19–21] The crystalline morphology is controlled by the cooling rate in that a low cooling rate corresponds to a large spherullite size with a high degree of molecular perfection. This correlation is clearly seen in Figure 1.[19] The interphase failure mechanisms are found also to be a direct reflection of the interphase adhesion mechanisms. The closely packed crystalline lamella interphase obtained from slow cooling gives rise to a high interface bond with a relatively brittle interface debonding failure, whereas the amorphous PEEK-rich interphase induced by fast cooling results in a low interface bond.

BACKGROUND

The evaluation of the relationship between the processing conditions and bulk mechanical properties of a thermoplastic matrix composite has received significant attention. In an early study on the effect of processing conditions, the tensile strength and fracture toughness of Thornal 300 carbon–PEEK composites in the transverse direction increased substantially if the holding time in the PEEK melt was increased.[5] A strong interface bond promoted by transcrystallization on the fiber surface at a long holding time was mainly responsible for this observation. A change in the cooling rate from 0.6 to 7°C/min had a negligible effect on the transverse properties. When the cooling rate was varied from 1 to 20°C/min, the longitudinal tensile/compressive strength and modulus of unidirectional APC2 laminates remained largely unchanged due to the expected dominance of fiber properties in that direction, whereas other properties such as the transverse and shear strength/modulus decreased to a varying extent. The reductions in the shear strength and modulus were most significant at 20%.[14] The explanation was invariably based on the crystallinity-sensitive neat PEEK properties in determining the mechanical performance of the composite. Similarly, the interlaminar shear strength (ILSS) of APC-2 decreased moderately from about 90 MPa at cooling rate of 0.5°C/min to 73 MPa at 200°C/min.[18] For the NCS-1025 laminate, fabricated from nonwoven symmetric bidirectional, unsized AS-4 fabrics and commingled PEEK filaments, a significant reduction in the ILSS was noted, especially at intermediate cooling rates between 20 and 63°C/min, where a sharp drop in the ILSS occurred, thus reaching only 45 MPa at 200°C/min.

In sharp contrast, there was little difference in the longitudinal tensile strength of $[\pm 45°]_s$ and quasi-isotropic IM6 carbon-PEEK laminates, as well as in the transverse tensile strength of unidirectional laminates when the laminates were processed at cooling rates of 1 and 50°C/min.[15] The only exception was the static failure strain of $[\pm 45°]_s$ laminates that showed up to a 50% increase at 50°C/min, similar to the previous findings,[10,12] attributable to the change in the matrix morphological structure.

The flexural properties also exhibited inconsistent results with respect to the cooling rate effect. While the longitudinal flexural strength had a significant dependency on the cooling rate with more than a 30% reduction for the quenched APC-2 laminates when compared to the slow-cooled counterpart, the flexural modulus had little dependency on the cooling rate.[16] Rather different trends were reported for pultruded carbon–PEEK composites. Both the longitudinal flexural strength and modulus decreased with an increasing cooling rate.[22,23] Meanwhile, the differences in the flexural strength and modulus caused by different cooling rates decreased gradually with an increasing loading angle relative to the fiber direction.[22] Therefore, there was virtually no difference between the transverse flexural strength and the modulus measured for slow-cooled and quenched APC-2 laminates with crystallinity about 35 and 10%, respectively. This anomaly was attributed to the difference in the residual stress state affected by the transcrystallinity. The transcrystalline layer formed on the fiber surface improved the longitudinal composite strength significantly. As a result, the longitudinal fatigue life of the slow-cooled laminates was also higher, up to three orders of magnitude, than that of the quenched counterpart. However, no direct correlation was found between the interphase modulus or the bond strength and the processing conditions.

Apart from the foregoing changes in the mechanical properties, the cooling rate also has a significant influence on the dimensional characteristics of a laminate. A high cooling rate produced a small curvature, corresponding to a large residual stress in nonsymmetric (0°/90°) laminates, because the internal stresses generated cannot be relaxed during fast cooling.[15,17] However, cooling rates less than 100°C/min were shown to have little effect on the curvature.[17] A high cooling rate also tended to induce a high void content, especially in areas exposed to a low processing pressure, which is detrimental to delamination resistance, and the annealing process had a negligible healing effect on voids.[24]

The foregoing literature survey found that, although many studies have been made to characterize the important mechanical behavior of a composite with respect to crystallinity, there was little consistency on the effect of the cooling rate.

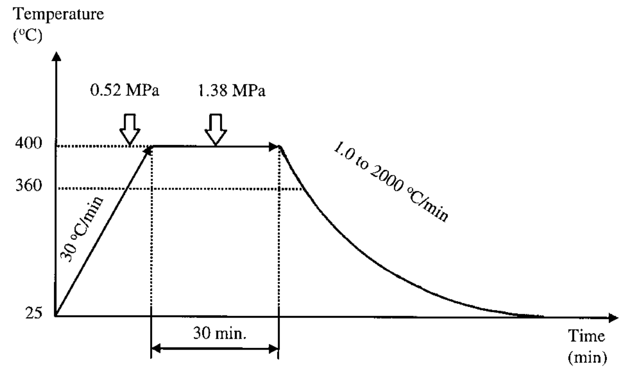

Figure 2 Temperature and pressure history during molding of the carbon fiber/PEEK composite.

A fundamental understanding of relative contributions by the interphase and the bulk matrix properties to the composite mechanical properties is of particular interest, but has never been addressed properly. Such a knowledge base is especially useful from the viewpoints of designing optimal processing conditions for balanced composite mechanical properties. Following our previous study of interphase adhesion, interlaminar fracture, and impact fracture resistance,[19–21] this study was designed to provide fundamental relationships among the interface adhesion, crystallinity, and bulk in-plane mechanical properties of composites. Ultimately, the aim is to establish an optimal processing cooling rate window for balanced mechanical and fracture characteristics.

EXPERIMENTAL

All composite specimens employed in the present study were prepared from APC-2 prepregs that contained continuous AS4 carbon fiber of 64% by volume and a PEEK matrix supplied by Fiberite, Inc. (Hong Kong, China). Laminates of 150 × 150 mm square were prepared by hand lay-up of 16 plies of prepreg, which were then consolidated using a matching metallic mold. The mold was pressed at 400°C and a pressure of 1.38 MPa for 30 min in a programmable hot press (Moore Hydraulic Press), which was equipped with built-in coolant channels. The details of the processing conditions are schematically shown in Figure 2.

Compressed air or cold water was supplied through the channels to obtain cooling rates from 1 to 80°C/min. Cooling rates between 100 and 1000°C/min were achieved by cooling the mold between cold aluminum plates after wrapping

Table I Summary of the Tensile Test Results and Crystallinity of Neat PEEK Resin

	Cooling Rate (°C/min)					
	1	80	160	600	1000	2000
Property	Mean ± SD	Mean ± SD	Mean ± SD	Mean ± SD	Mean ± SD	Mean ± SD
Tensile strength (MPa)	108.5 ± 5.0	93.8 ± 9.0	92.5 ± 3.5	71.7 ± 10.4	57.5 ± 3.5	53.8 ± 3.3
Tensile modulus (GPa)	4.6 ± 0.5	—	4.0 ± 0.3	3.7 ± 0.1	3.3 ± 0.2	3.0 ± 0.2
Failure strain (%)	3.0 ± 1.4	9.8 ± 1.4	7.9 ± 3.0	—	115 ± 7.1	183.3 ± 5.8
Crystallinity (%)	38	30	28	26	19	17

with polyimide films of different thicknesses. Cooling rates above 1000°C/min were achieved by quenching the mold directly in a water bath of ambient temperature. A Datapaq tracker with thermocouples embedded in the mold was used to monitor the temperature profile during cooling. The cooling rates reported here were calculated for the temperature range from 400 to 100°C, assuming that the PEEK crystallization under 100°C was negligible.[25] Since all fabricated laminates were equal to or thinner than 2 mm, it was assumed that the PEEK morphology did not vary appreciably throughout the bulk cross section.[26] The crystallinity of neat PEEK resin was measured using a differential scanning calorimeter (DSC). Neat PEEK resin sheets were also prepared for the mechanical tests.

Three types of mechanical tests were carried out: namely, tensile tests (ASTM D-3039) to determine strengths and moduli in both the longitudinal and transverse directions, three-point flexural tests (ASTM D-790) to determine the strengths and moduli in both the longitudinal and transverse directions, and short-beam shear tests (ASTM D-2344) to determine the ILSS. The laminates were cut into rectangular specimens for the tensile, three-point flex, and short-beam shear tests using a diamond-coated circular saw. These tests were performed on an MTS 858 universal testing machine with crosshead speeds of 1, 0.85, and 1.3 mm/min, respectively. The span-to-depth ratios in short-beam shear and three-point flexural tests were 4 and 16, respectively. The strengths and moduli were calculated from the maximum stress and the slope of the stress–strain curve. The fracture surfaces of specimens were examined using a scanning electron microscope (Cambridge Stereoscan 200) to study the failure mechanisms affected by the interface and bulk matrix properties.

RESULTS AND DISCUSSION

Tensile and Flexural Properties

Effect of Cooling Rate

A summary of the tensile properties as well as the degree of crystallinity of neat PEEK resin is presented in Table I, while comparisons of strengths and moduli for different loading directions are presented as a function of the cooling rate in Figures 3 and 4. As expected, the higher the cooling rate, the greater were all these mechanical properties. Except for the longitudinal tensile strength and modulus, which followed expected dominance by the fiber properties, the other mechanical properties exhibited high sensitivity to the cooling rate. The transverse tensile strength sharply decreased when the cooling rate was changed from 1 to 120°C/min, followed by a moderate decrease with a further increasing cooling rate. The flexural properties were shown to be even more sensitive to the cooling rate than were the transverse tensile properties.

Superimposed in Figure 3(a,b) are the longitudinal tensile strength and the Young's modulus of the composites calculated based on the simple rule of mixtures (ROM) using a tensile strength equal to 3.584 MPa[27] and a modulus E_f equal to 234.4 GPa[28] for the AS4 carbon fibers. For the whole range of the cooling rate studied, the ROM predictions were 6–20% higher than were the experimental modulus values and 48–58% higher than were the experimental strength values. This is expected because the ROM equation is a theoretical upper bound of the tensile properties, assuming that the fiber/matrix interface bonding is perfect and variations arising from imperfect fiber alignment, local nonhomogeneities, the void content, and the Poisson effect are neglected.[29] The differences between the ROM predictions and

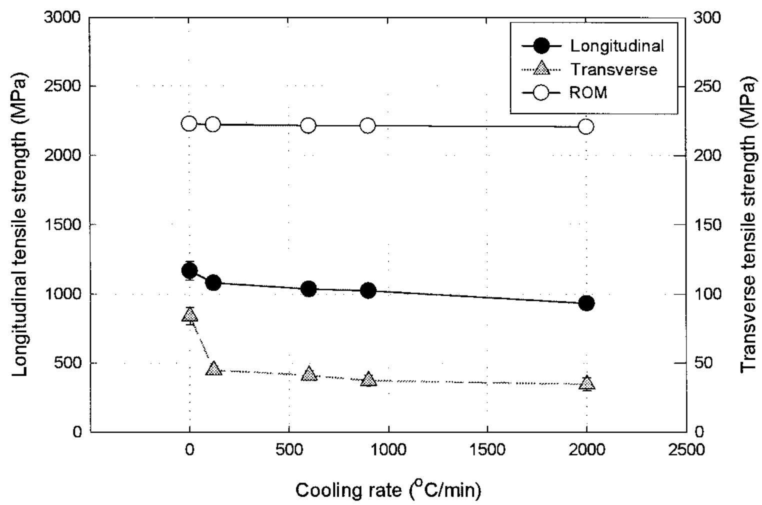

(a)

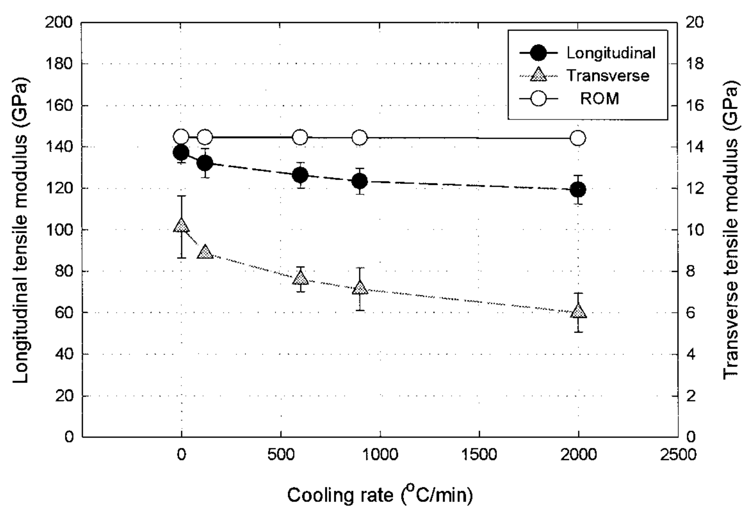

(b)

Figure 3 Variations of the (a) tensile strength and (b) modulus of carbon fiber/PEEK matrix composites with the cooling rate in the longitudinal and transverse directions.

the experimental results gradually increased with an increasing cooling rate, indicating a predominant influence of the interface bond strength on the longitudinal strength and modulus of the composites. Variations in the neat matrix properties had only negligible influence on the ROM prediction.

It is interesting to note, for the flexural strengths, is that the effect of the cooling rate was more significant in the longitudinal direction than in the transverse direction. A similar result was reported previously[23] in that the longitudinal flexural strength and modulus of the composites with a higher crystallinity were significantly (say, by 25 and 8%, respectively) higher than those with a lower crystallinty. The difference decreased gradually with an increasing loading angle relative to the fiber axis, leading to virtually no difference when the unidirectional composites were loaded in the transverse direction. The high flexural strength of the composites processed at 1°C/min is clearly associated with high flexural stiffness. The strong interphase adhesion and the PEEK matrix allowed the composite to sustain

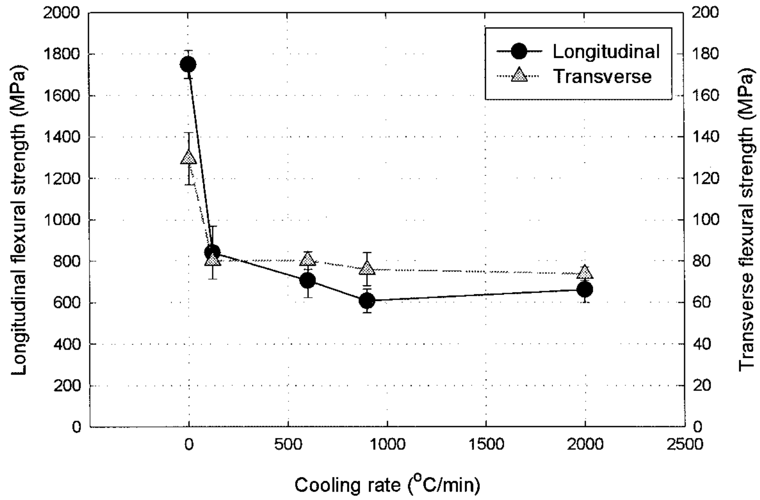

(a)

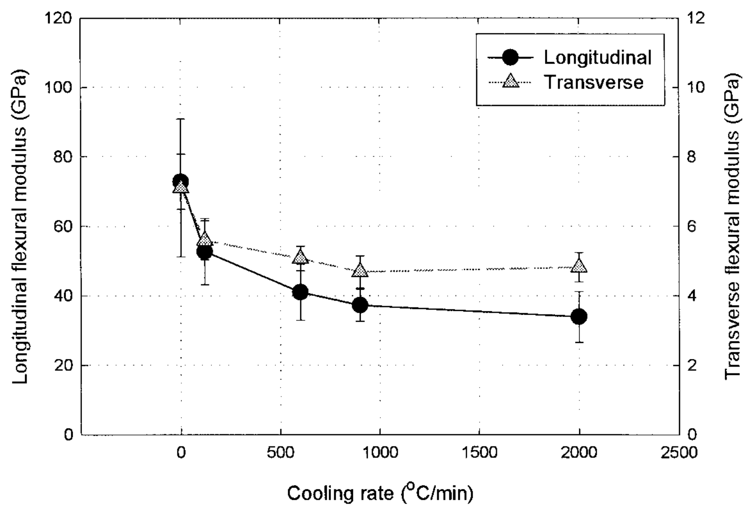

(b)

Figure 4 Variations of the (a) flexural strength and (b) modulus of carbon fiber/PEEK matrix composites with the cooling rate in the longitudinal and transverse directions.

larger flexural loads, but the brittle interphase and matrix did not allow large deformation. At cooling rates above 120°C/min, however, the amorphous-rich PEEK matrix became unable to sustain the applied strain, in particular, on the compression side when loaded in flexure. Coupled with a weak fiber–matrix interface bond strength, the weak compressive strength of the AS-4 carbon fibers—much weaker in compression than in tension—caused the composite to fail prematurely, impairing substantially the flexural strength. Another possible explanation may be due to the complex failure modes arising from the nonuniform compressive, tensile, and shear stress states in the three-point flexural configuration where critical stresses are confined within a small local volume, especially under the loading point. The high nonlinearity of the load-displacement curves observed for these composites partly confirms the above explanations, especially due to the premature compressive failure of the fibers and the local stress concentrations under the loading point.

Representative SEM fractographs of the longitudinal flexure specimens are shown in Figure 5, which reveals interesting features in the slow- and fast-cooled composites. There was an obvious change in the failure mode across the fracture surface: A distinct line separates the ragged and

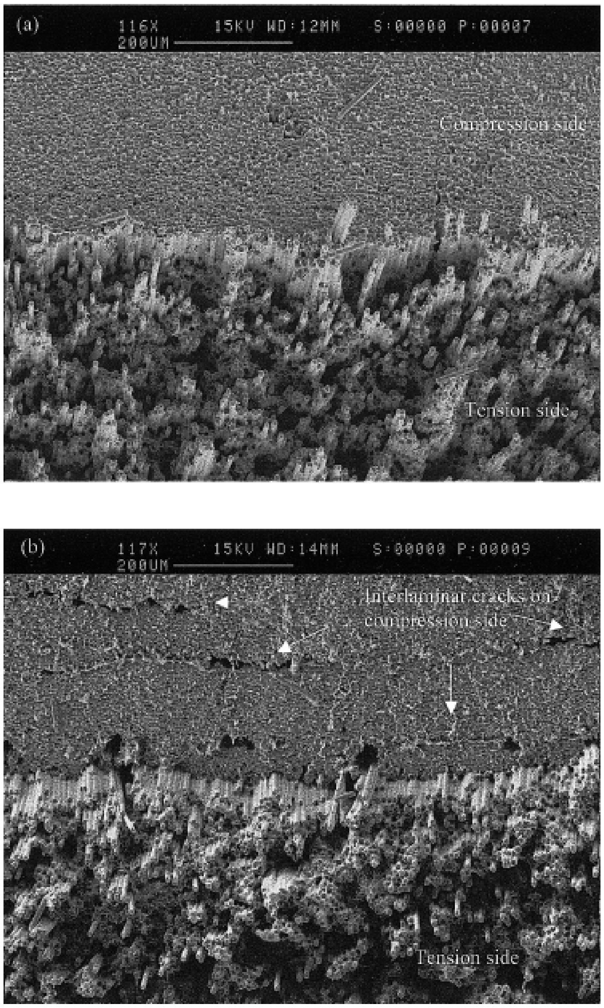

Figure 5 SEM fractographs taken from the longitudinal flexure specimens cooled at (a) 1°C/min and (b) 2000°C/min. Arrows indicate delaminations.

smooth fracture surfaces that correspond to areas subjected to tension and compression, respectively, during flexure. Fracture surfaces in the tension side were generally similar for both the slow- and fast-cooled specimens: The ragged surface contained mainly pulled-out fiber bundles.[30–32] More importantly, a distinguishable feature was revealed on the compression side. When the interface shear strength (IFSS) was at its highest level, such as those processed at 1°C/min, delamination and the fracture occurred due mainly to flexural failure of the composite. Meanwhile, there were several delamination cracks running parallel to the line separating the tension and compression sides in the specimens processed at fast cooling rates. These delamination cracks are a direct reflection of the weak fiber–matrix interface adhesion and compliant PEEK matrix that caused the composite to fail prematurely due to microbuckling.

Effect of Loading Geometry

It was found that the tensile properties were, in general, higher than were the corresponding flexural properties, with the exception of the transverse strength, which deserves further discussion. The transverse flexural strength was higher, by about 30–40 MPa, than was the corresponding tensile strength. While the transverse flexural strength was higher than was the matrix tensile strength when the cooling rate was higher than about 500°C/min or at a very low cooling rate (i.e., 1°C/min), the reverse was true for the rest of the cooling rate. In view of the different general trends for the IFSS/matrix strength and the transverse strengths, it seems that there were other important factors, in addition to the IFSS and matrix strength, that played a significant role in determining the transverse strength. The singular stress concentration existing at the fiber–matrix interface in the vicinity of a free edge is one of these factors. Finite element analysis on a straight-sided transverse tensile specimen revealed that interface debonding at free edges is the predominant cause of failure initiation.[33] When the interface bond was sufficiently strong (e.g., at a cooling rate of 1°C/min), the stress concentration did not deteriorate the transverse strength much. However, with the substantially lowered interface bonds at higher cooling rates, cracks were easily initiated from the free edges due to the stress concentrations, leading to premature failure at low loads. The tensile test is obviously more sensitive to the presence of free-edge stress concentration than is the flexural test because the latter test involves both the tension and compression sides of the specimen. This may explain why the transverse flexural strength was always greater than was the transverse tensile strength, although the general trends against the cooling rate were similar. The cruciform loading geometry was developed recently to avoid the free-edge stress concentrations in straight-sided transverse tensile specimens.[34,35]

In support of the foregoing discussion, photographs of a series of specimens processed at different cooling rates are presented in Figures 6 and 7. The slow-cooled specimen failed catastrophically in a brittle manner with a crack propagating right through the specimen width once

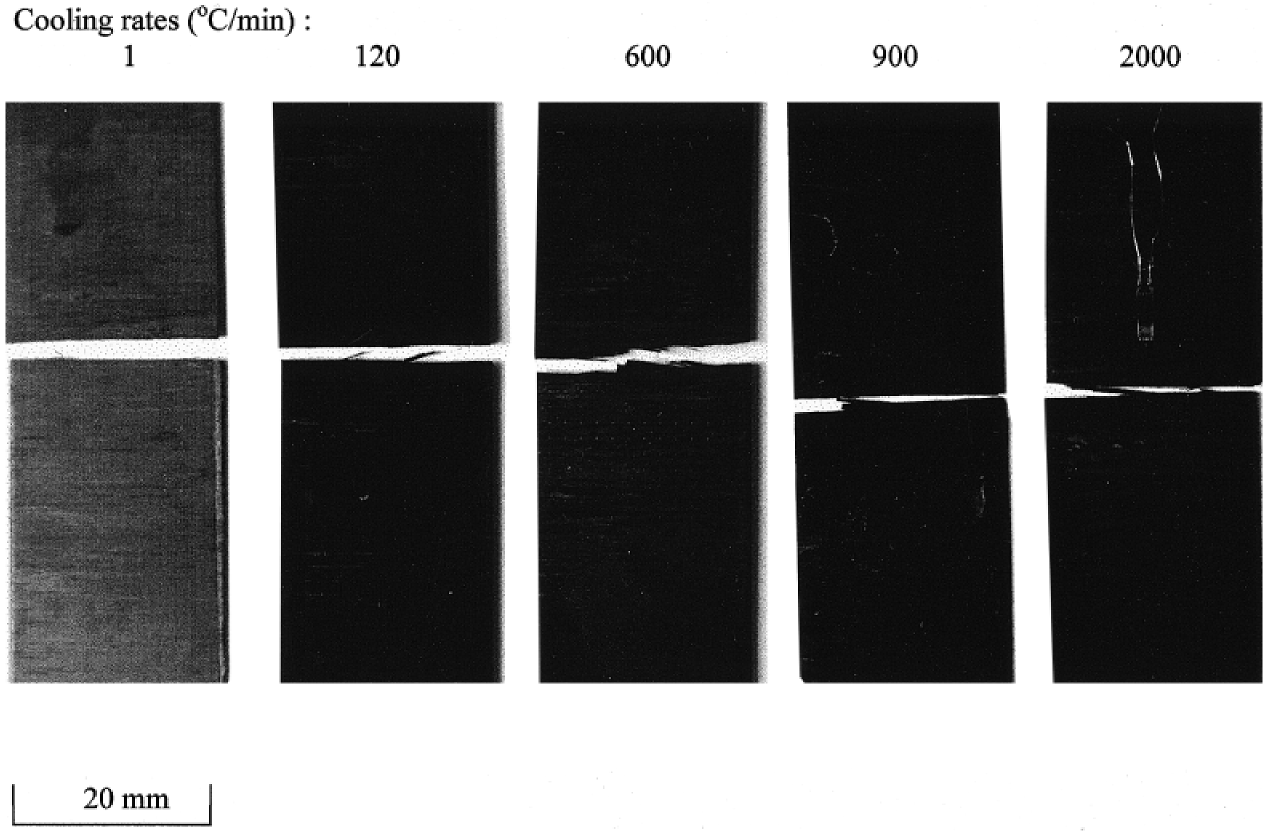

Figure 6 Photographs of fractured carbon fiber/PEEK matrix composite specimens after transverse tension tests.

the applied load reached a critical value. This resulted in a macroscopically flat, planar fracture surface. With an increasing cooling rate, the specimens displayed multiple-crack propagation as a result of fiber/matrix interface debonding initiated from the free edges due to the stress concentrations. Therefore, the fracture surface of these specimens became macroscopically more rugged with some bridged fibers. Judging from the fact that there was a sharp drop in the transverse tensile strength at a cooling rate right below 120°C/min, it seems that a transition of the fracture mode from unstable to interface-initiated more stable failure took place approximately at around this cooling rate.

The SEM fractographs presented in Figure 8 offer further evidence of the difference in failure mechanisms. Cohesive failure was dominant in the slow-cooled specimens [Fig. 8(a)] with the fiber surface being covered with a layer of crystalline PEEK. The distinctive fracture markings are reminiscent of PEEK spherullites that nucleate and grow preferentially on the carbon fiber surface.[36] The transcrystallites consist essentially of crystalline lamellae that are radially oriented on the fiber surface where the protospherullite is actually a sheaflike structure.[37] It was proposed recently[3,4] that the transcrystalline layer could contribute significantly to the composite strength and modulus when the chain axis in the polymer is preferentially oriented along the fiber axis. The appearance of cracking across the center of spherullites suggests that the failure was primarily caused by interlamellar slip and deformation, which provided great resistance to crack propagation due to the strong interactions between the PEEK chains and the fiber surface. This observation correlates well with the micromechanical characteristics in terms of the IFSS, interface morphology, and stiffness, as presented in our previous study.[19] On the contrary, the weak interfacial bond and high matrix ductility obtained at high cooling rates produced a fracture surface of relatively clean, debonded fibers and some matrix plastic yielding [Fig. 8(b)]. Adhesive failure was dominant in the microscopic scale due to the

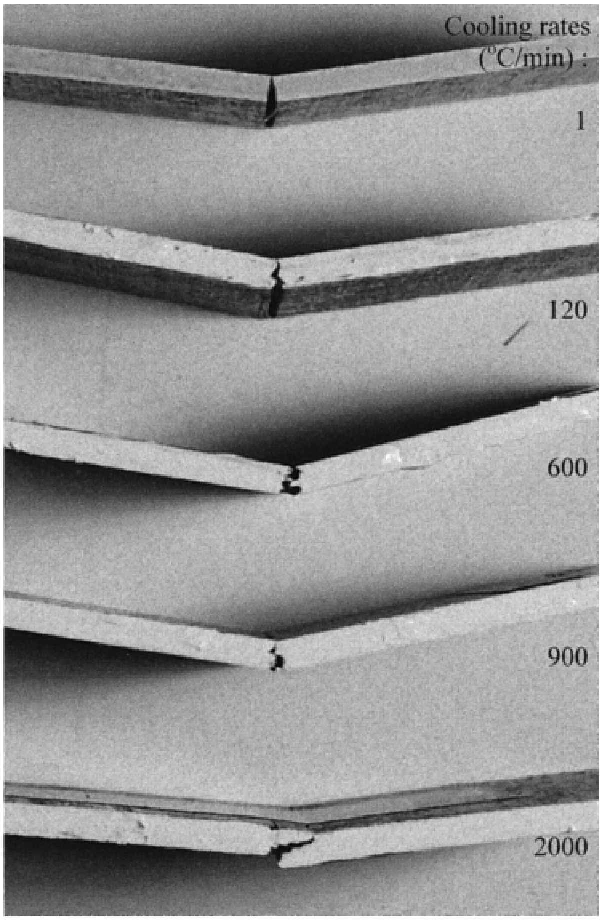

Figure 7 Photographs of fractured carbon fiber/PEEK matrix composite specimens after transverse flexure tests.

weak interface adhesion between the carbon fiber and the amorphous-dominated matrix.

Interlaminar Shear Strength

A strong correlation exists between the ILSS and IFSS with respect to the cooling rate: The higher the cooling rate, the lower the ILSS and IFSS, as shown in Figure 9. Also superimposed in Figure 9 are data for the crystallinity as a function of the cooling rate. Both the ILSS and IFSS decreased rapidly when the cooling rate was increased from 1°C/min to about 600°C/min, but further increase of the cooling rate beyond 600°C/min did not vary these interface parameters much. Meanwhile, the crystallinity decreased continuously following a large drop at a very low cooling rate. Worth noting is that the dependence of ILSS and IFSS on the cooling rate was functionally very similar in view of approximately proportional variations of these two strengths. The IFSS was consistently 20–30% higher than was the ILSS at a given cooling rate, as, in part, a reflection of the differences in the nature and loading geometry of the test.

Distinctive features were detected from the fracture surface of short-beam shear test specimens, as shown in Figure 10. At a slow cooling rate, a significant part of the fibers was covered with a layer of semicrystalline PEEK resin [Fig. 10(a)], as a result of the strong fiber/matrix interface bond. The adhering matrix displayed limited plastic deformation due to the high elastic modu-

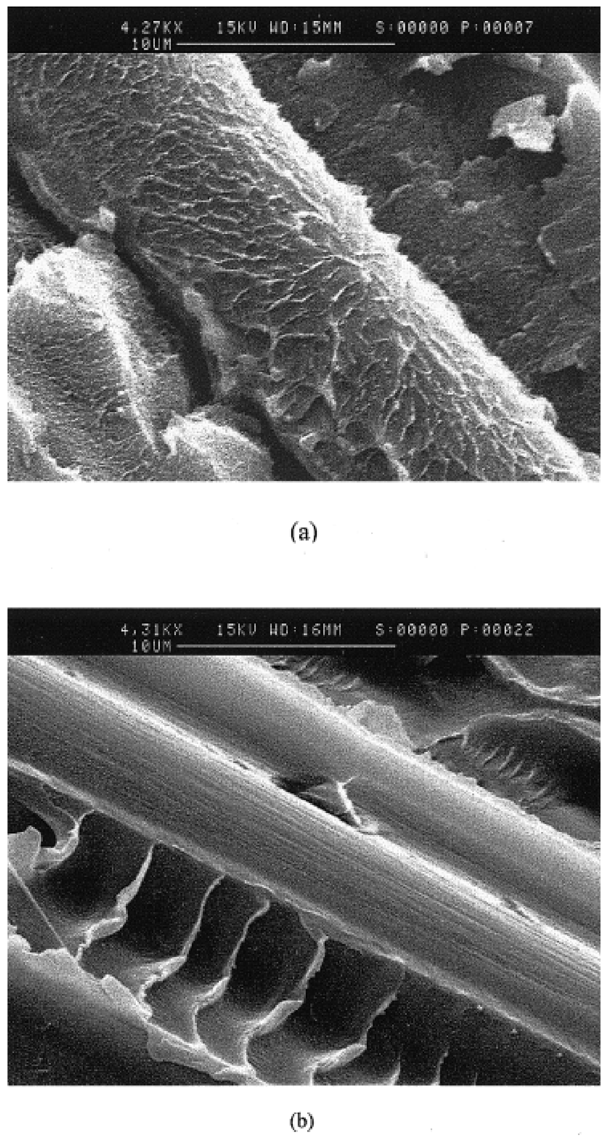

Figure 8 SEM fractographs taken from the tensile side of fracture surface of transverse flexural specimens cooled at (a) 1°C/min and (b) 1800°C/min.

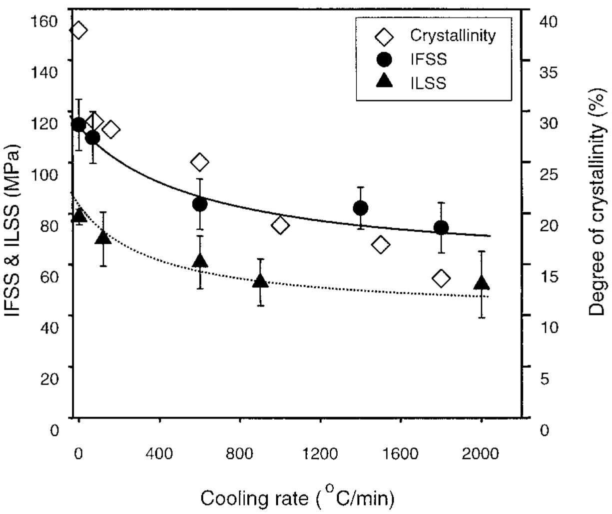

Figure 9 ILSS, IFSS, and degree of crystallinity plotted as a function of the cooling rate.

lus and low ductility of the resin with a high degree of crystallinity. With an increasing cooling rate, the PEEK matrix became more compliant/soft and ductile due to the lower degree of crystallinity, allowing more significant plastic deformation before failure [Figs. 10(b–d)]. However, the inherently weak fiber/matrix interface adhesion resulted in relatively easy debonding. Of note is that no significant changes in the fracture morphology were observed when the cooling rate was increased from about 600 to 2000°C/min, which is essentially consistent with the trend of both IFSS and ILSS for the same range of cooling rates. In summary, Figure 11 presents schematics of interlaminar shear failure mechanisms that are dependent on the crystallinity, ductility of the matrix, and the interface bond strength.

Sensitivities to Interface Adhesion and Matrix Strength

It was shown in the preceding section that the cooling rate significantly affects all the mechanical properties studied through its effect on the properties of the matrix material and the interface adhesion. These two parameters are, in turn, determined by the degree, morphology, and structure of the crystallinity surrounding the fiber and in the bulk matrix. It would be very useful to know to what extent these two parameters influence the mechanical properties of the composite. Therefore, all these mechanical properties of the composites are presented in a normalized form against both the normalized IFSS and the normalized matrix tensile strength, as shown in Figures 12 and 13. Only the mean data are plotted to avoid complexity of interpretation.

There are a few points of interest that can be taken from these plots. First, the correlations of the mechanical properties to these two parameters were basically similar in a general trend and magnitude, suggesting that both the fiber–matrix interface adhesion and the matrix strength are almost equally important. Second, with the exception of the longitudinal tensile strength, the other in-plane strengths had similar relations with the IFSS and matrix tensile strength. The longitudinal tensile strength clearly exhibited a linear variation with these parameters over the whole

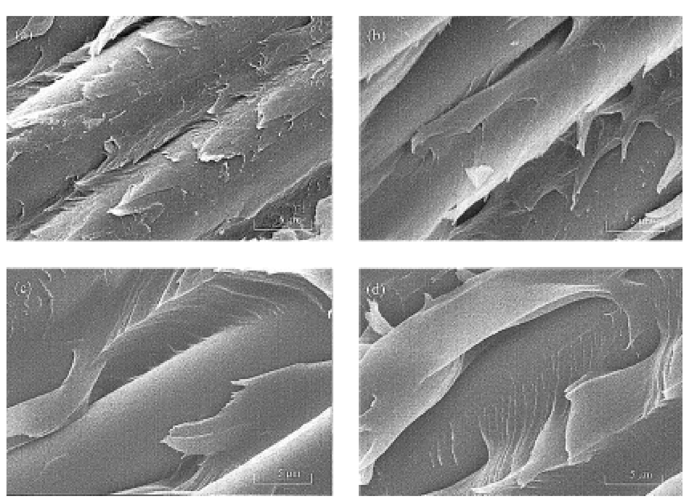

Figure 10 SEM fractographs of short-beam shear test specimens processed at the cooling rates of (a) 1°C/min, (b) 120°C/min, (c) 900°C/min, and (d) 2000°C/min.

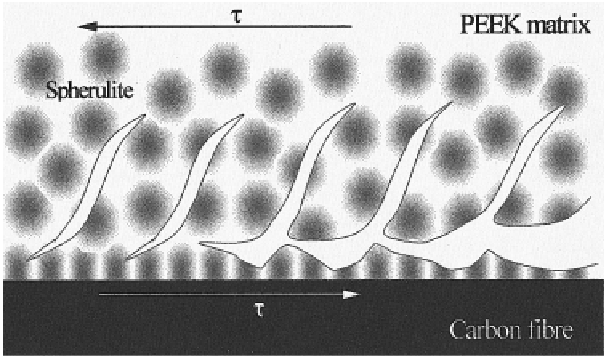

(a)

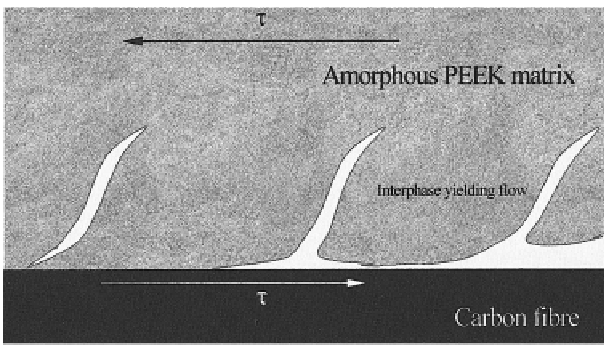

(b)

Figure 11 Schematics of interlaminar shear failure mechanisms in carbon fiber/PEEK matrix composites cooled at (a) 1°C/min and (b) 2000°C/min.

wide spectrum of the cooling rate, confirming the dominance of the fiber properties, even at the lowest cooling rate. Meanwhile, the interphase and matrix properties also played an important role, although minor to the fiber properties. There were discontinuities for the other normalized in-plane strength data, mainly because of the much lower strength values for all cooling rates at or above 120°C/min than for those measured at 1°C/min. Even so, the rate of variation was similar for all in-plane strength data. Third, it is very interesting to note that there is approximately a 1:1 linear relationship among the ILSS, IFSS, and matrix tensile strength for the whole range of cooling rates studied. A careful examination of Figure 13 reveals that the IFSS is slightly closer to the 1:1 proportionality than is the matrix strength, suggesting more dominance of the former property in determining the ILSS. The data points against the matrix strength were scattered above the proportionality line, particularly for the specimens corresponding to high cooling rates. This may indicate that the influence of the matrix properties diminishes and the interface properties become more dominant to determine the ILSS at high cooling rates.

It is also highlighted that cooling rates above 600°C/min had little influence on all mechanical

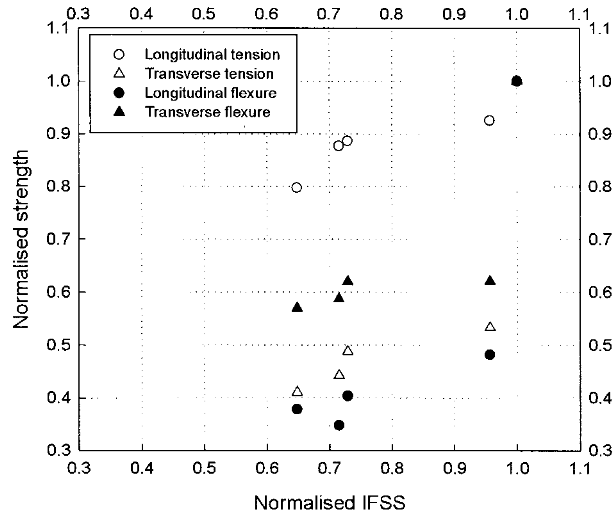

(a)

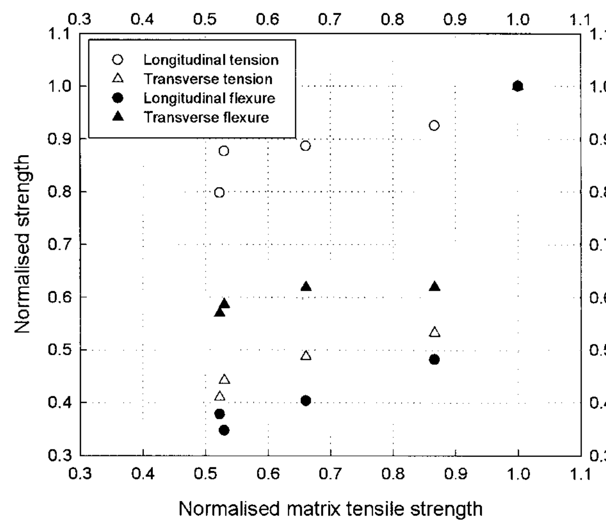

(b)

Figure 12 Plots of normalized strength versus (a) normalized IFSS and (b) matrix tensile strength. All data represent those normalized with the values obtained at the slowest cooling rate studied (i.e., 1°C/min).

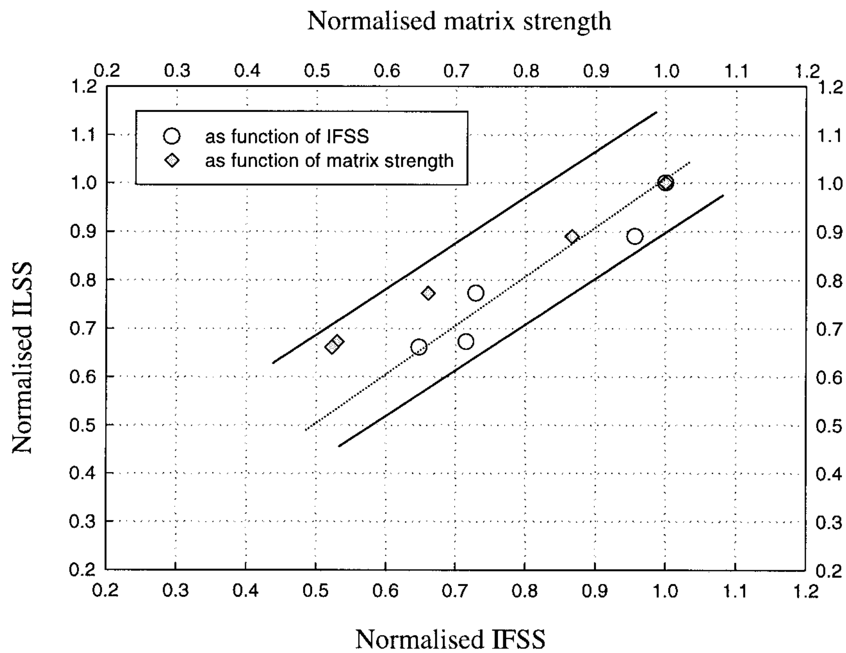

Figure 13 A plot of normalized ILSS versus normalized IFSS and matrix tensile strength. All data represent those normalized with the values obtained at the slowest cooling rate studied (i.e., 1°C/min).

properties measured in tension, flexure, or interlaminar shear. The similarities in the mechanical properties and the fracture surface morphologies of the composites processed at cooling rates above 600°C/min suggest that the low matrix strength and the low IFSS were almost fully realized in the composites obtained at 600°C/min. Therefore, the proportion of the decrease in the tensile, flexural, and interlaminar shear strengths, as a result of the decrease in the matrix tensile strength and the IFSS from the medium to the lowest levels, is much smaller than that observed at a lower cooling rate.

CONCLUSIONS

An experimental study was carried out to determine the effect of the processing cooling rate on the mechanical properties of carbon fiber/semicrystalline PEEK matrix composites in tension, flexure, and interlaminar shear. The rate of cooling from the molding temperature affected the fiber/matrix adhesion and the bulk matrix properties, through a dominant effect on the degree, morphology, and structure of the crystallinity. These characteristics, in turn, controlled the unidirectional composite mechanical properties, while the fiber properties remain unchanged. Major findings from the experimental studies are highlighted in the following.

The tensile, flexure, and interlaminar shear properties all exhibited high sensitivity to the cooling rate. The longitudinal tensile strength and modulus showed the least sensitivity among those mechanical properties, due to the fiber property dominance. The effect of the cooling rate was much more significant on the longitudinal flexural strength than on the longitudinal tensile strength due mainly to the greater roles played by the fiber–matrix interface bond and matrix strength for the composite strength in bending than in longitudinal tension. The transverse flexural strength of the composites was always much higher than was the transverse tensile strength. The singular stress concentrations existing at the fiber–matrix interface of specimen's free edges were mainly responsible for the premature failure in the tensile test.

The ILSS varied with the cooling rate in a very similar manner to the IFSS, that is, the higher the cooling rate, the lower were these properties. The normalized plots confirmed approximately the 1:1 linear dependence of the ILSS on the IFSS. The correlations of the in-plane and interlaminar properties measured in this study to the

IFSS and matrix strength were basically similar in trend and magnitude. This indicates that the interface bond strength and the matrix are equally important for the in-plane and interlaminar properties.

The Research Grant Council (CERG HKUST719/95E) and the Area of Excellence Grant (AoE97/98.EG14) of Hong Kong University of Science & Technology (HKUST) financially supported this project. Most experiments were conducted with support from the Advanced Engineering Materials Facility (AEMF) and the Materials Characterisation & Preparation Facilities of HKUST.

REFERENCES

1. Cogswell, F. N. Thermoplastic Aromatic Polymer Composites; Butterworth–Heinemann: Oxford, 1992.
2. Advanced Thermoplastic Composites: Characterisation and Processing; Kausch, H. H.; Legras, R., Eds.; Hanser: Munich, Germany, 1993.
3. Stern, T.; Marom, G.; Wachtel, E. Composites A 1997, 28, 437–444.
4. Nuriel, H.; Klein, N.; Marom, G. Compos Sci Technol 1999, 59, 1685–1690.
5. Lee, Y.; Porter, R. S. Polym Eng Sci 1986, 26, 633–639.
6. Ishida, H.; Bussi, P. In Structure and Properties of Composites, Materials Science and Technology: A Comprehensive Treatment; Chou, TW, Ed.; VCH: New York, 1991; Vol. 13, pp 339–379.
7. Seferis, J. C. Polym Compos 1986, 7, 158–169.
8. Cebe, P.; Chung, S. Y.; Hong, S. D. J Appl Polym Sci 1987, 33, 487–496.
9. Talbott, M. F.; Springer, G. S.; Berglund, L. A. J Compos Mater 1987, 21, 1056–1081.
10. Curtis, P. T.; Davies, P.; Partridge, I. K.; Sainty, J P. In Processings Sixth International Conference on Composite Materials (ICCM 6/ECCM 2); Elsevier: London, 1987; Vol. 4, pp 401–412.
11. Lustiger, A.; Uralil, F. S.; Newaz, G. M. Polym Compos 1990, 11, 65–75.
12. Cantwell, W. J.; Davies, P.; Kausch, H. H. Compos Struct 1990, 14, 151–171.
13. Saiello, S.; Kenny, J.; Nicolais, L. J Mater Sci 1990, 25, 3493–3496.
14. Vautey, P. SAMPE Q 1990, 21, 23–28.
15. Davies, P.; Cantwell, W. J.; Jar, P. Y.; Richard, H.; Neville, D. J.; Kausch, H. H. In Composite Materials: Fatigue and Fracture; O'Brien, T. K., Ed.; ASTM STP 1110; ASTM: Philadelphia, 1991; pp 70–88.
16. Russell, J. D.; Curliss, D. B. In Proceedings of the 23rd SAMPE Technical Conference 1991; pp 91–103.
17. Unger, W. J.; Hansen, J. S. J Compos Mater 1993, 27, 108–137.
18. Vu-Khanh, T.; Denault, J. J Reinforc Plast Compos 1993, 12, 916–931.
19. Gao, S. L.; Kim, J. K. Composites A 2000, 31, 517–530.
20. Gao, S. L.; Kim, J. K. Composites A 2001, 32, 763–774.
21. Gao, S. L.; Kim, J. K. Composites A 2001, 32, 775–785.
22. Astrom, B. T.; Larsson, P. H.; Hepola, P. J.; Pipes, R. B. Composites 1994, 25, 814–821.
23. Tregub, A.; Harel, H.; Marom, G.; Migliaresi, C. Compos Sci Technol 1993, 48, 185–190.
24. Manson, J. E.; Schneider, T. L.; Seferis, J. C. Polym Compos 1990, 11, 114–120.
25. Blundell, D. J.; Osborn, B. N. Polymer 1983, 24, 953–958.
26. Lee, W. I.; Springer G. S. J Compos Mater 1987, 21, 1017–1055.
27. Madhukar, M. S.; Drzal, L. T. J Compos Mater 1992, 26, 310–333.
28. Waterbury, M. C.; Drzal, L. T. In Controlled Interphases in Composite Materials; Ishida, H., Ed.; Elsevier: New York, 1990; pp 731–739.
29. Madhukar, M. S.; Drzal, L. T. J Compos Mater 1991, 25, 958–991.
30. Shikhmanter, L.; Eldror, I.; Cina, B. J Mater Sci 1988, 24, 167–172.
31. Kim, J. K.; Mai, Y. W. J Mater Sci 1991, 26, 4702–4720.
32. Kim, J. K.; Mai, Y. W. Compos Sci Technol 1991, 41, 333–378.
33. Tandon, G. P.; Kim, R. Y.; Warrier, S. G.; Majumdar, B.S. Composites B 1999, 30, 115–134.
34. Gundel, D. B.; Majumdar, B. S.; Miracle D. B. Scr Met Mater 1995, 33, 2057–2065.
35. Kim, J. K.; Mai, Y. W. In Comprehensive Composite Materials: Vol. 3, Metal Matrix Composites; Clyne, T. W., Vol. Ed.; Elsevier: Oxford, UK, 2000; pp 117–138.
36. Dixon, D. G. J Mater Sci Lett 1990, 9, 606–608.
37. Waddon, A. J.; Hill, M. J.; Keller, A.; Blundell, D. J. J Mater Sci 1987, 22, 1773–1784.